Facile H–D exchange in adsorbed methylidyne on Pt{110}–(1×2) and deuteration to gaseous methane

ARTICLE *in* THE JOURNAL OF CHEMICAL PHYSICS · DECEMBER 2001

Impact Factor: 2.95 · DOI: 10.1063/1.1410387

3 AUTHORS, INCLUDING:

Qingfeng Ge
Southern Illinois University Carbondale

129 PUBLICATIONS **2,733** CITATIONS

SEE PROFILE

Facile H–D exchange in adsorbed methylidyne on Pt{110}–(1×2) and deuteration to gaseous methane

D. T. P. Watson, Q. Ge, and D. A. King
Department of Chemistry, Lensfield Road, University of Cambridge, Cambridge CB2 1EW, United Kingdom

(Received 5 June 2001; accepted 21 August 2001)

Hydrogen–deuterium exchange in adsorbed methylidyne, CH_a, on Pt{110}–(1×2) has been studied for the first time using supersonic D_2/H_2 molecular beams, which provides new insights into the reversible hydrogenation of adsorbed hydrocarbon fragments. The exchange reaction is extremely facile at surface temperatures of 350–450 K and proceeds via a Langmuir–Hinshelwood reaction between D_a and a CH_a fragment to produce gas phase H_2 and HD. The $CD_a + H_a$ (i.e., reverse) reaction was also studied and was found to proceed more slowly. Both exchange reactions were successfully modeled and the difference in reaction rates is explained using zero point energy differences alone. Finally, we demonstrate that with high incident D_2 fluxes CH_a can be completely deuterated to produce gaseous CHD_3 and CD_4. © *2001 American Institute of Physics.*
[DOI: 10.1063/1.1410387]

I. INTRODUCTION

Interest in the reactivity of C_1 hydrocarbon fragments on metal surfaces arises from their presence as reactive intermediates in technologically important processes such as Fischer Tropsch synthesis[1,2] and the oxidative coupling of methane. Most studies to date have concentrated on CH_{3a}, due to the simplicity in preparing pure adlayers, by either thermal decomposition of methyl halide precursors[3–7] or using a CH_3 radical source.[8,9]

The rehydrogenation and exchange of CH_{3a} has been studied by many groups.[3–5,8] Using CH_3I as a precursor, Zaera *et al.*[3–5] found that rehydrogenation to methane occurs with high selectivity if either D_2 or H_2 is coadsorbed, and dehydrogenation to C_a is only a minor pathway. When D_2 is co-adsorbed, the major product is CH_3D which is formed by the elementary reaction, $CH_{3a} + D_a \rightarrow CH_3D$. However, measurable amounts of methane products produced by multiple H–D exchange reactions were observed and are attributed to a rapid CH_{2a}/CH_a interconversion. Using a methyl radical source to produce CH_{3a} adlayers on Pt{111}, Fairbrother *et al.*[8] found that CH_{3a} is rehydrogenated exclusively to CH_3D. This competes with dehydrogenation which is favored at low CH_{3a} and D_a precoverages. They found no evidence for H–D exchange in CH_{3a} during rehydrogenation. The discrepancies between the findings of the two groups may be due either to perturbation of the process in the presence of coadsorbed I^- or to the presence of a small amount of CH_{2a} not observed by Fairbrother *et al.*[8]

To date, CH_a exchange and rehydrogenation has not been studied experimentally. This is primarily due to the fact that until recently[10] there was no way of preparing a sufficiently pure CH_a adlayer. From DFT slab calculations performed by Michaelides and Hu on Pt{111}[11] and by Nørskov and co-workers on Ni{111},[12] activation energies for CH_a hydrogenation to CH_{2a} of 94 kJ mol^{-1} and 70 kJ mol^{-1} were reported, respectively. Here we provide an experimental basis for benchmarking calculations of this kind.

The importance of quantum mechanical (QM) tunneling in H transfer reactions is still a matter for debate. Several investigators have used tunneling to explain the dependence of alkane sticking probabilities over transition metals on incident kinetic energy.[13,14] In fact, Harris and Luntz[15] have provided a theoretical treatment for methane dissociative adsorption where H tunneling is the rate determining step for C–H bond activation. The above studies are by no means conclusive and the studies which have provided the most insight into this question have involved determining the magnitude of the kinetic isotope effect (KIE): In a normal kinetic isotope effect, the reaction rates of C–H dissociation, k_H, and C–D dissociation, k_D, are determined solely by the different depths of the zero point energy in the potential energy well, and hence by the consequently different activation energies for dissociation (note the expected value for k_H/k_D will also depend on the surface temperature). By contrast, if tunneling of H or D through the activation barrier to dissociation is significant, the different probabilities of tunneling for H or D due to their different masses, will also affect k_H/k_D.

Yata and Madix[16] found that $k_H/k_D = 3.1$ for simple C–H bond cleavage in ethylene on Pt{111} and Watson *et al.*[17] found a normal kinetic isotope effect for methylidyne C–H bond cleavage on Pt{110}–(1×2); these results can be explained using zero point energy differences alone. Fairbrother *et al.*[8] found that CD_{3a} dedeuteration occurs about 5–7 K above CH_{3a} dehydrogenation indicating $k_H/k_D > 1$, again a normal isotope effect. Methyl rehydrogenation experiments performed by Harrison and Ukraintsev[18] showed a small isotope effect ($k_H/k_D = 1.3$) measured at 240 K, which also suggest that tunneling across the activation barrier is insignificant for both methane dissociation and formation. In this paper we study the $CD_a + H_a$ and $CH_a + D_a$ exchange reactions using molecular beam reaction spectroscopy and determine the importance of QM tunneling for both these reactions.

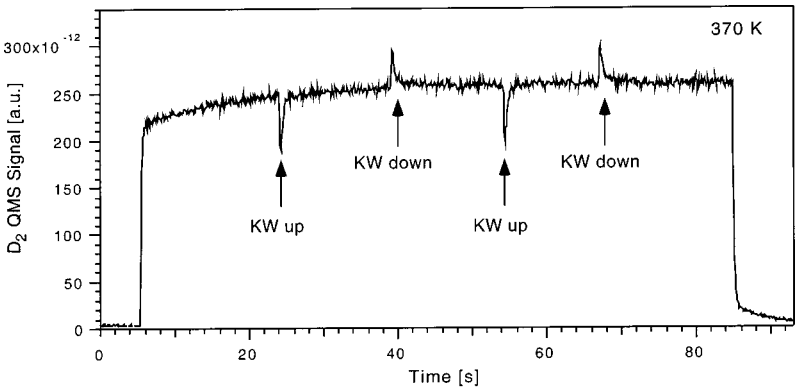

FIG. 1. KW experiment to measure the net sticking probability of D_2 at a surface temperature of 370 K and beam flux of 0.024 ML s^{-1}.

II. EXPERIMENTAL DETAILS

The experimental apparatus is described in detail elsewhere.[19] The sample is mounted centrally on a manipulator in an ultrahigh vacuum chamber with a base pressure of $<2\times10^{-10}$ mbar. The molecular beam is sourced by supersonic expansion through a 50 μm nozzle, skimmed, differentially pumped and collimated before entering the sample chamber. An inert King and Wells (KW) flag just in front of the crystal is used to control the dosing time and to measure sticking probabilities.[20] A source stage flag can also be inserted to prevent impingement on the KW flag. The surface temperature (T_s) is monitored by a crystal-mounted thermocouple referenced to an electronic ice-point and is regulated by programmed resistive heating. The partial pressures of up to 16 individual gases can be monitored using a fixed quadrupole mass spectrometer (QMS) situated behind the crystal.

The Pt sample, 11 mm diameter by 1 mm thick, was cut to within 0.1° of the {110} plane. Initial cleaning of the crystal was achieved by repeated cycles of ion sputtering, annealing, and oxygen treatment. Routine cleaning consisted of annealing at 1240 K followed by exposure to oxygen for 5 minutes while cooling from 1100 to 950 K and then annealing for 15 minutes at 950 K. This procedure yields a clean Pt{110}–(1×2) surface which gives a sharp LEED pattern and oxygen thermal desorption spectra that are in good agreement with the literature.[21] The CH_4 and O_2 used were >99.9995% and 99.995% pure, respectively, as quoted by the suppliers [Messer (UK) Ltd.]. The supersonic methane beams used in these experiments had a composition of 8% CH_4–92% He and the nozzle was heated to 790 K, giving the methane molecular beam a translational energy of 580 meV, estimated on the basis of an ideal supersonic expansion.

The H_2 and D_2 beams employed were produced using a room temperature nozzle. The flux, which was calibrated using a spinning rotor gauge (SRG), was determined using the QMS pressure rise in the main chamber while beaming and could be varied by adjusting the pressure behind the nozzle. All coverages are quoted in monolayers (ML) (1 ML≡9.22 $\times10^{14}$ molecules cm^{-2}). The coverages were determined using the King and Wells technique[20] and by comparison of temperature programmed desorption (TPD) areas with earlier studies.[22,23]

III. RESULTS AND DISCUSSION

A. The reactive D_2 sticking probability on a clean Pt{110}–(1×2) crystal

Before the exchange process was studied, the adsorption/desorption kinetics of H_2 and D_2 on the clean Pt{110}–(1×2) surface were examined. At surface temperatures below the H_2 desorption temperature of 310 K,[24] the initial disso-

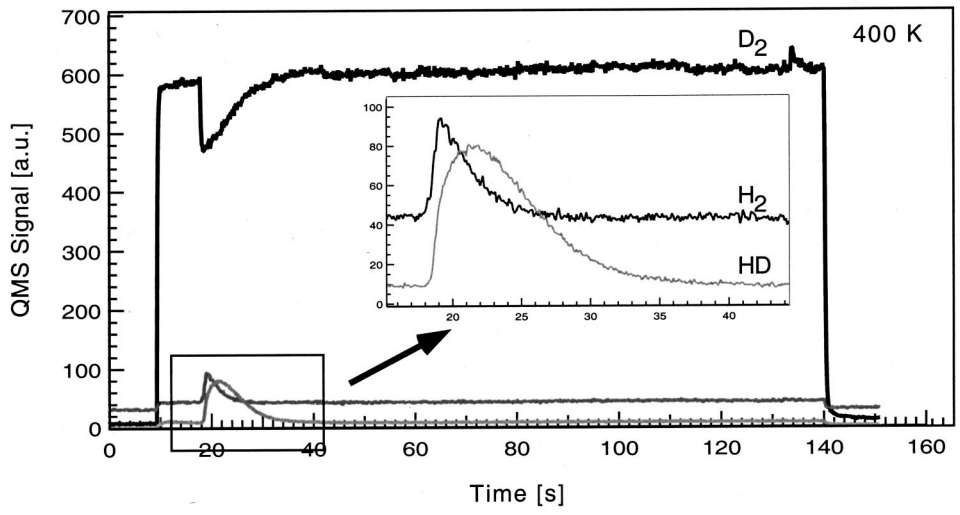

FIG. 2. The D_2 exchange of H in CH_a to produce H_2 and HD. The D_2 beam flux is 0.062 ML s^{-1}, the CH_a coverage is 0.045 ML and the surface temperature is 400 K.

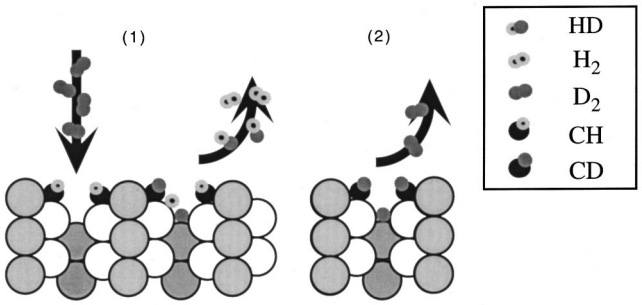

FIG. 3. Schematic of D_2 exchange of H in CH_a; (1) the D_2 beam impinges, dissociates and exchanges, producing HD and H_2; (2) D_2 beam turned off.

ciative sticking probability on the clean surface is 0.3 for each isotope.[25] At surface temperatures close to and above the desorption temperature, where desorption becomes significant, the KW technique[20] measures a net sticking probability.[26] Figure 1 shows a typical KW sticking experiment for a D_2 beam at a surface temperature of 370 K. After ~5 s the source stage flag is opened and the D_2 beam impinges directly against the inert KW flag. The randomly scattered D_2 molecules cause a rise in the D_2 pressure, which is measured using the fixed QMS. After 24 s the KW flag is raised and the beam impinges directly against the crystal. The scattered intensity is reduced because a fraction of the D_2 molecules sticks. This drop in pressure is used to determine an initial net sticking probability of 0.23. After 40 s the KW flag is lowered to block the beam from impinging directly against the crystal. There is a small D_2 pulse which has the same area and hence the same number of molecules as the drop in pressure when the flag was raised. The flag was raised and lowered again after 55 and 66 s, respectively, with identical responses. This shows that the processes taking place at the surface are completely reversible. The observed response can be explained if we consider the following equilibrium which exists above the desorption temperature:

$$D_2 \underset{k_d}{\overset{sF_{D_2}}{\rightleftharpoons}} 2D_a, \tag{1}$$

where s, F_{D_2}, and k_d are the absolute sticking probability, D_2 flux at the crystal and the rate constant for desorption, respectively. When the D_2 beam impinges directly against the crystal the D_2 pressure (flux) at the crystal increases. According to le Chatelier's principle this causes the equilibrium to shift to the right: some D_2 molecules dissociatively adsorb, increasing the surface concentration of atomic D_a. When the KW flag is lowered, the D_2 beam is blocked and thus the D_2 pressure at the crystal is reduced. The equilibrium shifts to the left and a pulse of D_2 is observed. The identical response on opening and closing the KW flag again shows that the process is completely reversible. This method was used to determine the net sticking probability at a surface temperature of 400 K and it was found to be 0.13.

B. Hydrogen–deuterium exchange in adsorbed methylidyne

In our earlier work[10] we demonstrated that a pure methylidyne (CH) adlayer could be formed on Pt{110} by adsorbing methane from a supersonic molecular beam source at a crystal temperature of 370 K. Saturation exposure yields an ordered $c(2\times4)$ overlayer at a coverage of 0.25 ML. If the crystal temperature during CH_4 exposure is lowered to 300 K, the adlayer consists of CH and H adatoms, but heating to 370 K results in recombinative desorption of the H adatoms as H_2. At temperatures above 400 K the CH adlayer begins to decompose, producing gaseous H_2 and residual carbon. It was concluded that adsorbed CH is the only stable surface dissociation product over the surface temperature range from 350 to 400 K;[10] at these temperatures the remaining H adatom coverage is negligible.

The H in CH_a can be exchanged using a D_2 beam at a surface temperature of 400 K. The CH_a adlayer is prepared by dosing the 0.42ML s^{-1} He/CH_4 beam described in the experimental section for 25 s, at a surface temperature of 370 K. A D_2 beam with a flux of 0.062 ML s^{-1} is employed to initiate the exchange reaction. In the results shown in Fig. 2, at 10 s the source stage flag is raised and the D_2 is randomly scattered from the inert KW flag, resulting in a rise in D_2 pressure. The KW flag is raised after 18 s which leads to an instantaneous decrease in the D_2 pressure. The D_2 initial reactive sticking probability is increased from 0.13 on the clean surface, as described in Sec. III A, to 0.21. The time required for the net sticking probability to return to zero (~17 s) is much greater than for the clean surface (less than

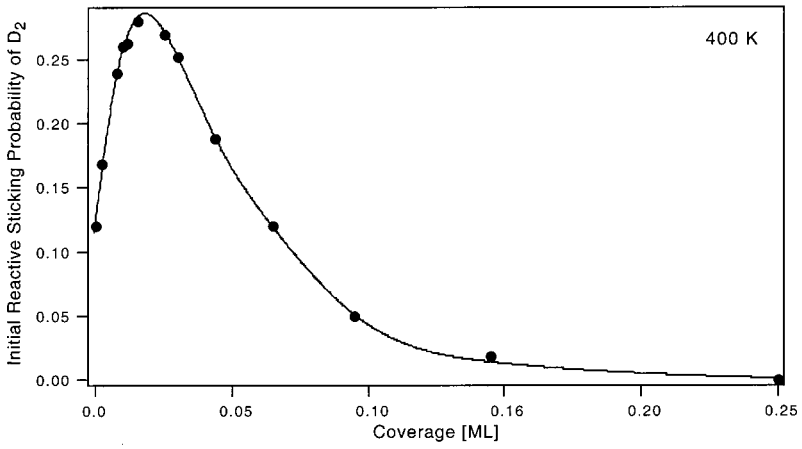

FIG. 4. Initial reactive D_2 sticking probability as a function of CH_a coverage, at a D_2 beam flux of 0.062 ML s^{-1} and a surface temperature of 400 K.

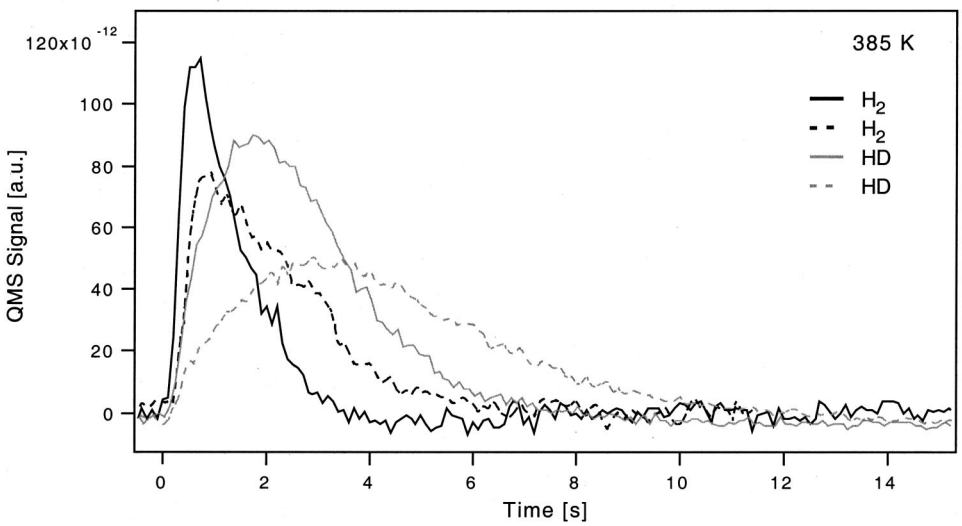

FIG. 5. D_2 exchange of H in CH_a, to produce H_2 and HD, with D_2 fluxes of 0.08 ML s^{-1} (solid lines) and 0.04 ML s^{-1} (dashed lines). The CH_a coverage and surface temperature were 0.05 ML and 370 K, respectively.

2 s, Fig. 1). The H_2 and HD partial pressures increase while exchange is taking place. These two product profiles have completely different peak shapes, as shown magnified in the inset to Fig. 2. The H_2 signal rises to a maximum almost instantaneously (~1 s), while the HD signal rises more slowly to a maximum after 4 s and slowly decays to the base value. There is also a small pulse of D_2 when the KW flag is lowered after ~135 s; as for the clean surface, it is due to recombination and desorption of atomic D_a when the D_2 beam is removed.

The processes taking place on the surface during exchange are shown schematically in Fig. 3. The D_2 adsorbs dissociatively and exchanges with CH_a to produce atomic H_a, which can recombine with either H_a or D_a atoms to produce H_2 or HD, respectively. The implicit assumption that exchange is preceded by D_2 dissociation is justified below.

After exchange was complete, the crystal temperature was uniformly ramped at a rate of 6 K s^{-1} and the H_2, D_2, and HD partial pressures followed. These products arise from decomposition of CH and CD on the surface. After exchange with a high flux D_2 beam the only product is D_2, with a peak maximum at 480 K. However, if the crystal temperature is not ramped immediately, a small HD signal is obtained. This is due to exchange of CD_a with background H_2.

The deuterium exchange reaction was repeated with different initial precoverages of CH_a, at the surface temperature of 400 K. Figure 4 shows the variation of the D_2 initial reactive sticking probability with CH_a precoverage. The reactive D_2 dissociative sticking probability increases from 0.13 at close to zero CH coverage to a maximum of 0.28 at a CH coverage of 0.02 ML, then decreases to zero at CH_a saturation coverage. Here we note that D_2 must dissociate for exchange to take place. If the mechanism was Eley–Rideal, involving a reaction between incident D_2 and adsorbed CH_a, the sticking probability would increase continuously with CH_a coverage. Second, a reactive sticking probability of 0.28 at a CH coverage of 0.02 ML, which is nearly the same as that for the absolute sticking probability on the clean surface below the desorption temperature, i.e., at 300 K, shows that the reaction is extremely efficient. In fact, if we assume that at a CH_a coverage of 0.02 ML every D_2 that dissociates exchanges before it desorbs and that each CH_a blocks one site for D_2 adsorption, the reactive sticking probability is given by $s_0(1-0.02/0.25)^2=0.27$, which agrees within experimental error with the observed value of 0.28. At coverages below 0.02 ML there are not enough CH_a fragments to react with every D_2 that dissociates and D_2 recombinative desorption become more significant. Using this simple model we would expect the reactive sticking probability to drop as

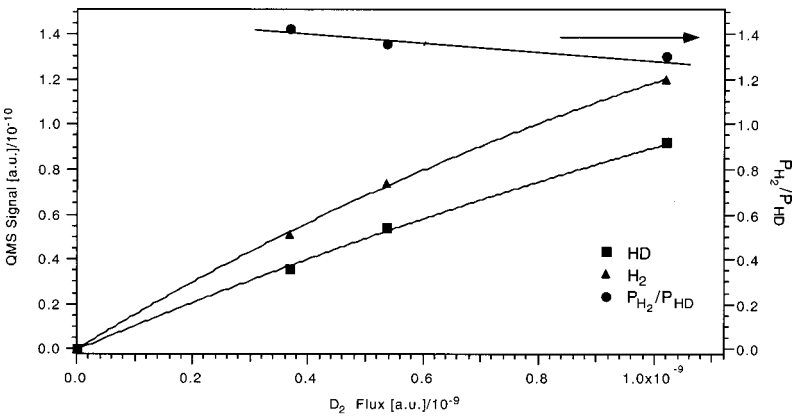

FIG. 6. The maximum rate of H_2 and HD production as a function of D_2 flux at a surface temperature of 385 K (left-hand axis). The corresponding ratio of maximum H_2 and HD production rates is also included (right-hand axis).

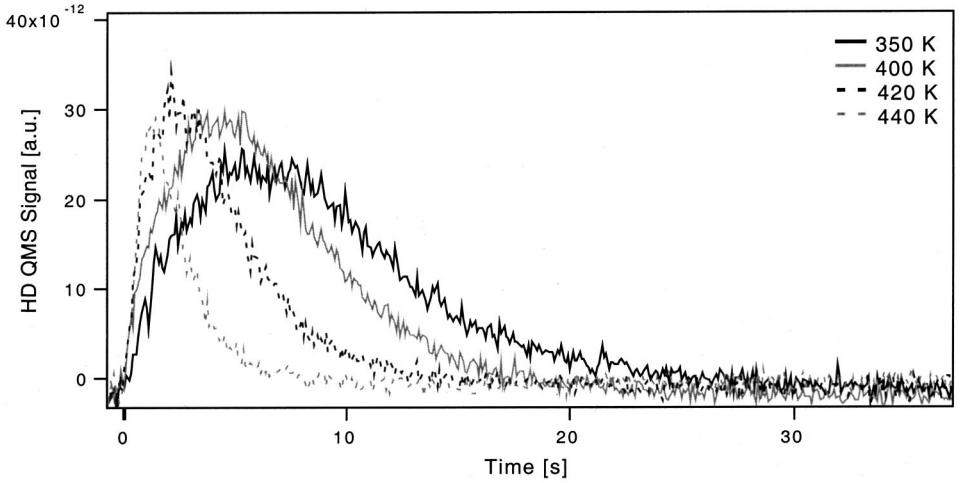

FIG. 7. HD produced by D_2 exchange of H in CH_a over the surface temperature range 350–440 K. The D_2 beam flux is 0.022 ML s^{-1} and CH_a precoverage is 0.05 ML. The CH_a precoverage decreases as the reaction temperature increases above 400 K as a result of the conversion of CH_a to C_a.

$(1-\theta_{CH})^2$ at coverages above 0.02 ML; as there is sufficient CH_a to react with all the dissociated D_2, CH_a simply acts as a site blocker to D_2 dissociation. However, the sticking probability drops off more quickly than expected, indicating that the energetics for the $CH_a + D_a$ exchange reaction and D_2 dissociative adsorption are coverage dependent.

C. Influence of D_2 flux and surface temperature on the $CH_a + D_a$ exchange reaction

We next examined the influence of D_2 flux on the $CH_a + D_a$ exchange reaction. The product profiles for the reaction of a 0.05 ML CH_a overlayer and a D_2 beam with fluxes of 0.08 ML s^{-1} and 0.04 ML s^{-1} can be seen in Fig. 5. The reaction rate increases when the D_2 flux, and hence the D_a coverage, are increased, while the peak shapes remain unchanged. The QMS signal at the H_2 and HD peak maxima are plotted versus the D_2 beam flux in Fig. 6. Again we see that increasing the D_2 beam flux increases the peak heights (rate) of both H_2 and HD. The ratio of the peak heights is also included and we find that the rate of HD production relative to H_2 is higher when the D_2 flux is increased. Clearly an increased D_a coverage increases the rate of HD production.

The effect of surface temperature on the product profiles over the temperature range 350–440 K are shown in Figs. 7 and 8. The CH_a adlayer had a coverage of 0.05 ML and the D_2 flux was 0.022 ML s^{-1}. Increasing the surface temperature from 350 to 400 K had very little effect on the temporal profiles of the H_2 and HD produced. The rate of the reaction increases slightly, with the HD peak maximum occurring after ~7 s at 350 K and ~5 s at 400 K while the H_2 peak remains unchanged. Increasing the surface temperature to 420 K produces a more noticeable change. There is some conversion of CH_a to C_a on heating to this temperature[10] before the exchange experiment is performed, as seen by the decrease in the H_2 and HD peak areas. The peak maxima for both H_2 and HD production occur after shorter amounts of time than at 400 K. At 440 K there is further conversion of CH_a to C_a and the exchange reaction is completed after about 7 s. To completely understand what is happening, we need to look at the corresponding D_2 reactive sticking probability curves, Fig. 8(b). In the temperature range 350–400 K the initial reactive sticking probability stays almost constant, at 0.18. As the temperature increases, the reactive sticking probability increases to 0.30 at 440 K. The reason for this is the increasing conversion of CH_a to C_a. At 440 K

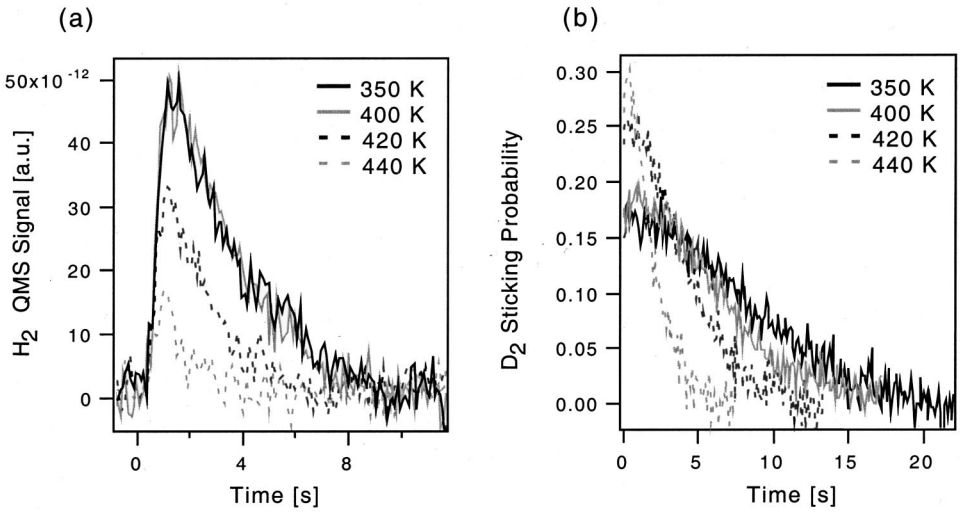

FIG. 8. (a) H_2 produced by D_2 exchange of H in CH_a over the surface temperature range 350–440 K. The D_2 beam flux is 0.022 ML s^{-1} and the CH_a precoverage is 0.05 ML. (b) Reactive D_2 sticking for the same reaction.

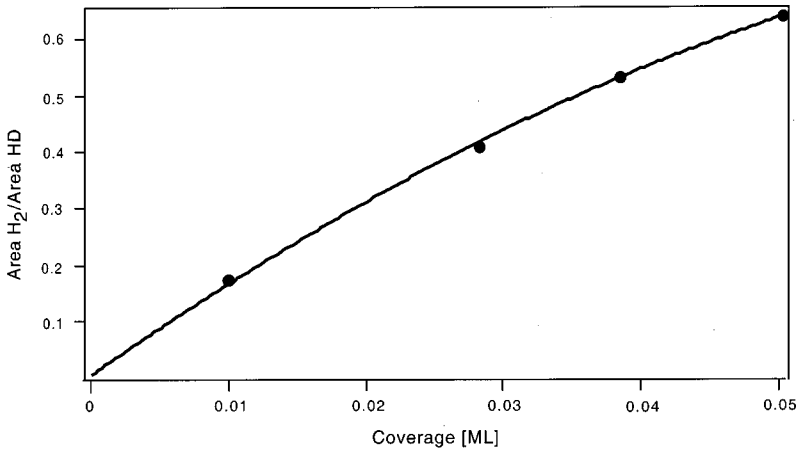

FIG. 9. Ratio of the amount of H_2 to HD produced by the D_2 exchange of H in CH_a as a function of CH_a coverage. The D_2 beam flux is 0.022 ML s^{-1}.

the CH_a coverage decreases to 0.014 ML, which is near the maximum in the D_2 reactive sticking versus CH_a coverage curve, Fig. 4. Therefore, the large increase in rate between 400 and 440 K can be simply attributed to the increased D_2 sticking probability and hence the D_a coverage. This shows that the surface reaction is not very sensitive to surface temperature in this regime and must have quite a low activation energy.

Figure 9 shows the ratio of the areas of the H_2 produced divided by that of the HD produced versus the the CH_a coverage (corrected for conversion of CH_a to C_a). We find that the relative amount of HD produced increases with decreasing CH_a coverage and extrapolates to 100% HD as the CH_a coverage approaches zero. No quantitative conclusion can be reached from the shape of the curves, as the experiments were not performed at constant temperature. However, the results are consistent with our model: as the CH_a coverage decreases the amount of H_a produced decreases and an exchanged H_a atom has a greater chance of combining with a D_a atom, increasing the relative amount of HD.

D. H_2 exchange of D_a in CD_a: Relative rate and selectivity

The exchange reaction is completely reversible and can be driven in the opposite direction by beaming H_2 at a CD_a adlayer. However, the rate of the reaction is slower in this direction and the selectivity is completely different, with only a relatively small amount of D_2 being produced. Figure 10 shows a comparison of the exchange reaction in each direction using identical fluxes of D_2 and H_2. For the $CD_a + H_a$ exchange reaction the rate of the product formation reaches a maximum in less time than for the $CH_a + D_a$ reaction. However, the reaction takes almost twice as long to go to completion. The difference in reaction rates must be attributed either to zero point energy differences or to quantum mechanical tunneling of the H atom through the reaction barrier. We discuss this further below.

The reaction rate and selectivity for the $CD_a + H_a$ reaction were also investigated as a function of H_2 flux. Figure 11 shows the maximum rate of D_2 and HD production as function of H_2 flux. Again we find that the rate increases with

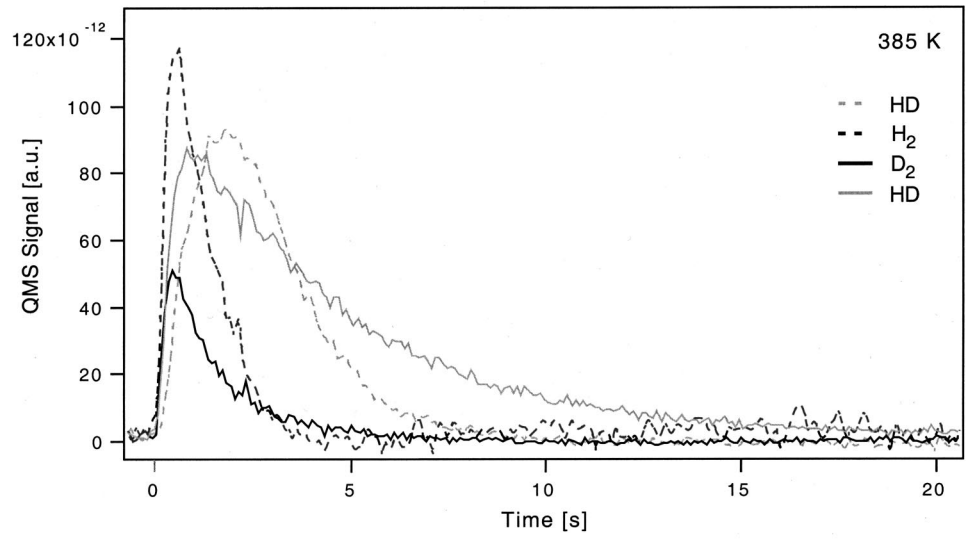

FIG. 10. Product profiles for the $CH_a + D_a$ (dashed lines) and $CD_a + H_a$ (solid lines) reactions at a surface temperature of 385 K. The H_2/D_2 flux is 0.08 ML s^{-1} and the CH_a/CD_a coverage is 0.05 ML.

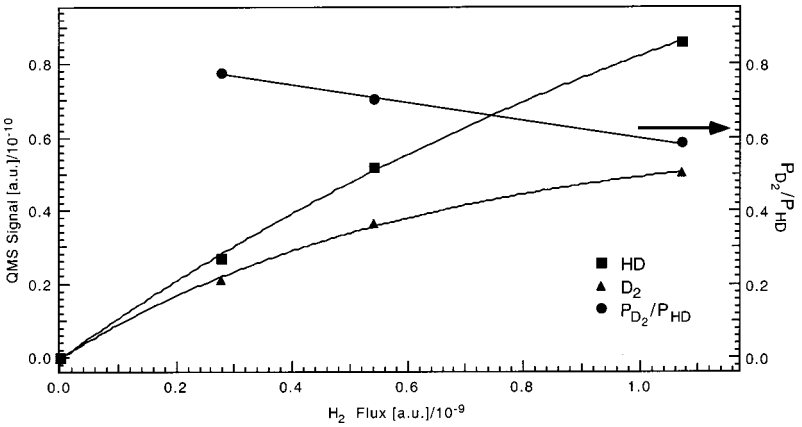

FIG. 11. Maximum rate of D_2 and HD production as a function of H_2 flux at a surface temperature of 385 K (left-hand axis). The ratio of the D_2 to HD maximum rates is also included (right-hand axis).

increasing flux. However, the rate of D_2 production seems to be approaching an asymptote value. The relative selectivity to D_2, determined by the ratio of the maximum rates is also included. We find that the fraction of D_2 produced decreases with increasing H_2 flux. This is also consistent with our model: the selectivity to D_2 decreases as the H_a coverage increases.

E. Rehydrogenation of CH_a to form gas phase CHD_3 and CD_4

Using a high flux D_2 beam ($\sim$1.2 ML s^{-1}) we found that CH_a can be completely deuterated to produce gas phase CHD_3 and CD_4. Figure 12 shows the rehydrogenation of a 0.12 ML CH_a adlayer at a surface temperature of 370 K. There is a small sharp CHD_3 peak and a CD_4 peak which rises sharply to a maximum and decreases slowly until the reaction is complete after about 500 s. The inset is the magnification of the first few seconds of the reaction. The CHD_3 maximum occurs after $\sim$1 s while the CD_4 maximum occurs after $\sim$7 s, by which time the rate of CHD_3 production is negligible. The exchange reaction to produce HD and H_2 (not shown here) is complete before the CD_4 signal reaches its maximum. These findings are consistent with a stepwise deuteration mechanism: i.e.,

$$CH_a + D_a \overset{1}{\rightleftharpoons} CHD_a + D_a \overset{2}{\rightleftharpoons} CHD_{2a} + D_a \overset{3}{\rightarrow} CHD_3(g).$$

Each of the surface steps is reversible, with $CD_a + H_a$ being an alternative product of step (1), i.e., the exchange reaction. CHD_3 is formed only if deuteration occurs without exchange taking place at any step. Therefore, the maximum in CHD_3 production occurs almost instantaneously (the first data point after the KW flag is raised), before exchange to CD_a is complete. We note that no C_2 species were observed in the gas phase.

To determine whether the CH_a adlayer was completely removed by deuteration, a titration method was employed. This involved heating the crystal to 700 K after deuteration and reacting the residual C_a with an O_2 beam to produce CO. The area under the CO trace is directly proportional to the amount of unreacted carbon on the surface. The titration experiment was repeated on a CH_a adlayer that had not been deuterated. Both the CO profiles are shown in Fig. 13. More than 95% of the surface CH_a was removed by deuteration.

These results confirm the earlier conclusion[10] that CH_a is the stable species of methane dissociation at 370 K. First, the observed CHD_3 and CD_4 products are consistent with stepwise deuteration of CH_a. Second, the absence of gas phase C_2 species and the virtually complete removal of the carbon-

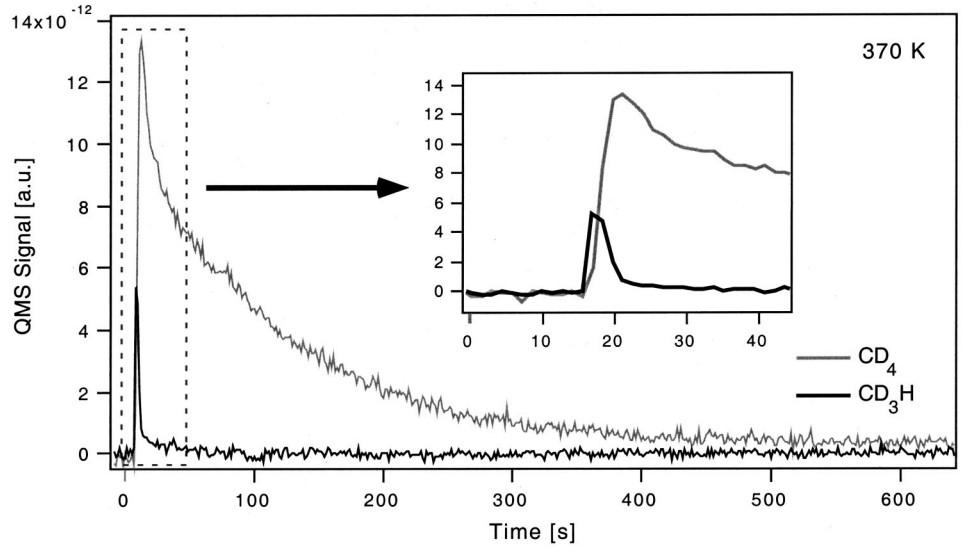

FIG. 12. Rehydrogenation of a 0.12 ML CH_a adlayer to produce CHD_3 and CD_4 using a D_2 beam of 1.2 ML s^{-1} flux at a surface temperature of 370 K. The inset is the first 20 s of the reaction magnified.

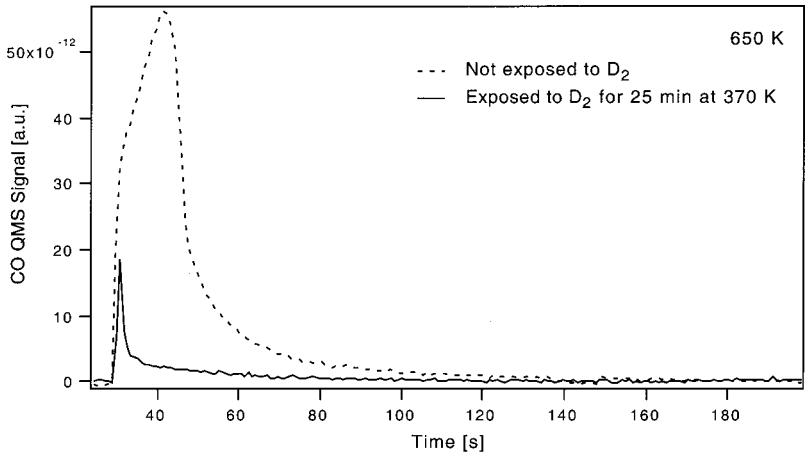

FIG. 13. Titration of C_a produced by CH_a dehydrogenation with an O_2 molecular beam at a surface temperature of 700 K, with (solid line) and without (dashed line) performing the rehydrogenation experiment.

aceous adlayer by deuteration shows that C_2 species are not present on the surface to a significant degree. If C_2 species were present on the surface, deuteration should lead to CCD_{3a}. We conclude that the adlayer consists of at least 95% CH_a.

CH_a dehydrogenates to produce to C_a and gas phase H_2 on heating to temperatures greater than 470 K.[10] It was found that carbon produced using this procedure could not be rehydrogenated under the conditions studied, namely D_2 fluxes as high as 1.2 ML s^{-1} and surface temperature range 250–700 K. This is consistent with the work of Smirnov *et al.*[27] on Pt{111}. They found that atomic carbon produced using a carbon deposition source could be rehydrogenated above 240 K. However, if the surface was preannealed to 500 K, the C_a could no longer be rehydrogenated and was attributed to the formation of unreactive carbon in the form of graphite.

IV. MODELING THE EXCHANGE REACTION

A. The model

The reaction was modelled using the following elementary reaction steps:

$$D_2 \underset{k_d}{\overset{s_0 F_{D_2}}{\rightleftharpoons}} 2D_a, \tag{2}$$

$$CH_a + D_a \underset{k_{-1}}{\overset{k_1}{\rightleftharpoons}} CD_a + H_a, \tag{3}$$

$$H_a + D_a \overset{k_d}{\rightarrow} HD, \tag{4}$$

$$2H_a \underset{s_0 F_{H_2}}{\overset{k_d}{\rightleftharpoons}} H_2, \tag{5}$$

where k_d, k_1, and k_{-1} are the rate constants for $H_2/D_2/HD$ desorption, the $CH_a + D_a$ reaction and the $CD_a + H_a$ reaction, respectively. F_{D_2}, F_{H_2}, and s_0 are the D_2 flux, H_2 flux and sticking probability. The first step is the reversible adsorption and dissociation of D_2 (2). The next step is the reversible exchange via CHD_a (3). The exchanged H_a adatoms can either react with D_a atoms to produce HD (4) or another exchanged H_a to produce H_2 (5). Since each HD or H_2 molecule that is produced is pumped away the reaction (in theory) can be driven to completion. (In practice, since background H_2 is always present in the chamber, the $CD_a + H_a$ exchange reaction always has a finite rate.)

Four coupled differential equations are used to describe the variation of adsorbate coverages:

$$\frac{d\theta_H}{dt} = -2k_d\theta_H^2 - k_d\theta_H\theta_D - k_{-1}\theta_{CD}\theta_H + k_1\theta_{CH}\theta_D + 2F_{H_s}s_0(1-\kappa\theta_{CH})^2, \tag{6}$$

$$\frac{d\theta_D}{dt} = -2k_d\theta_D^2 - k_d\theta_H\theta_D + k_{-1}\theta_{CD}\theta_H - k_1\theta_{CH}\theta_D + 2F_{D_2}s_0(1-\kappa\theta_{CH})^2, \tag{7}$$

$$\frac{d\theta_{CH}}{dt} = k_{-1}\theta_{CD}\theta_H - k_1\theta_{CH}\theta_D, \tag{8}$$

$$\frac{d\theta_{CD}}{dt} = -k_{-1}\theta_{CD}\theta_H + k_1\theta_{CH}\theta_D. \tag{9}$$

Here θ_x is the coverage of species x relative to the saturation coverage of CH_a at 370 K and κ is a correction factor which takes into account that every CH_a fragment may block more than one H_2/D_2 adsorption site. Weinberg and co-workers [24] found that on Pt{110}–(1×2) the desorption kinetics for H_2, D_2, and HD are the same within experimental error and that H_2 desorption was first order with an activation energy and pre-exponential factor which change with coverage. We found that for low H_2 pre-coverages on a clean surface, H_2

TABLE I. Parameters used in the model.

Reaction	Rate (s^{-1})	E_a (kJ mol^{-1})	ν (mol^{-1} cm^2 s^{-1})	Ref.
D_2/H_2 Flux	F_{D_2/H_2}	0.028 (ML s^{-1})		Calculated
$D_2 \rightarrow 2D_a$	s_0	0.3		25
	κ	1		This work
$2H_a \rightarrow H_2$	k_d	65	5.6×10^{-4}	24, 25
$2D_a \rightarrow H_2$	k_d	65	5.6×10^{-4}	24, 25
$D_a + H_a \rightarrow H_2$	k_d	65	5.6×10^{-4}	24, 25
$CH_a + D_a \rightarrow CD_a + H_a$	k_1	69.5	5.6×10^{-4}	This work
$CD_a + H_a \rightarrow CH_a + D_a$	k_{-1}	73.2	5.6×10^{-4}	This work

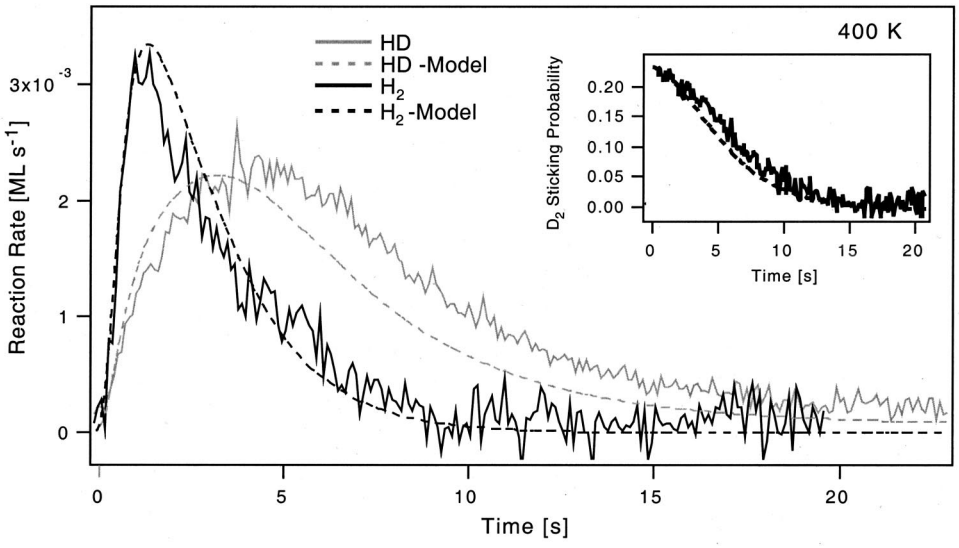

FIG. 14. Experimental (solid lines) and modeled (dashed lines) profiles of the H_2 and HD produced during the $CH_a + D_a$ reaction, for a CH_a precoverage of 0.04 ML and D_2 flux of 0.028 ML s^{-1}, at a surface temperature of 400 K. The inset shows the corresponding D_2 reactive sticking probability.

desorption is best described as a second order process with fixed kinetic parameters. Therefore, for simplicity in this model we describe the adsorption and desorption of H_2, D_2, and HD using second order Langmuirian behavior.

The above set of coupled differential equations cannot be solved explicitly and must be solved using numerical integration. The initial coverages and beam fluxes were determined experimentally. The parameters taken from the literature (where possible), are listed in Table I. The only unknowns were k_1, k_{-1}, and κ. Reasonable guesses were made for these unknown parameters and the system of coupled differential equations was solved numerically, using Fortran routines (NAG library). This yielded time dependent coverages for all the surface species. These were inserted into the following set of equations which describe the time dependent D_2 sticking probability (s_{D_2}), HD pressure (P_{HD}) and H_2 pressure (P_{H_2}):

$$s_{D_2} = s_0(1-\kappa\theta_{CH})^2 - \frac{k_d\theta_{D_2}^2}{F_{D_2}}, \tag{10}$$

$$P_{HD} = k_d\theta_D\theta_H, \tag{11}$$

$$P_{H_2} = k_d\theta_H^2. \tag{12}$$

The resulting profiles were compared to the experimentally determined curves and the parameters k_1, k_{-1}, and κ were varied until the best fit was obtained. In Fig. 14 the experimentally determined profiles and best fit theory profiles are shown for the exchange reaction at 400 K. The best fit parameters are included in Table I. The same procedure was applied to the reverse reaction, using the same parameters but different initial conditions (replacing the CH_a adlayer with a CD_a adlayer and the D_2 beam with a H_2 beam). The best fit is shown in Fig. 15. It is clear that there is a good quantitative fit for both directions using the same parameters.

We found that the model is insensitive to variations the absolute values of the rate constants to within ±50%, but extremely sensitive to the ratio of the rate constants for the forward (k_1) and reverse (k_{-1}) reactions. The insensitivity of the model to surface temperature is reflected in the experimental behavior. For this reason we were unable to use an

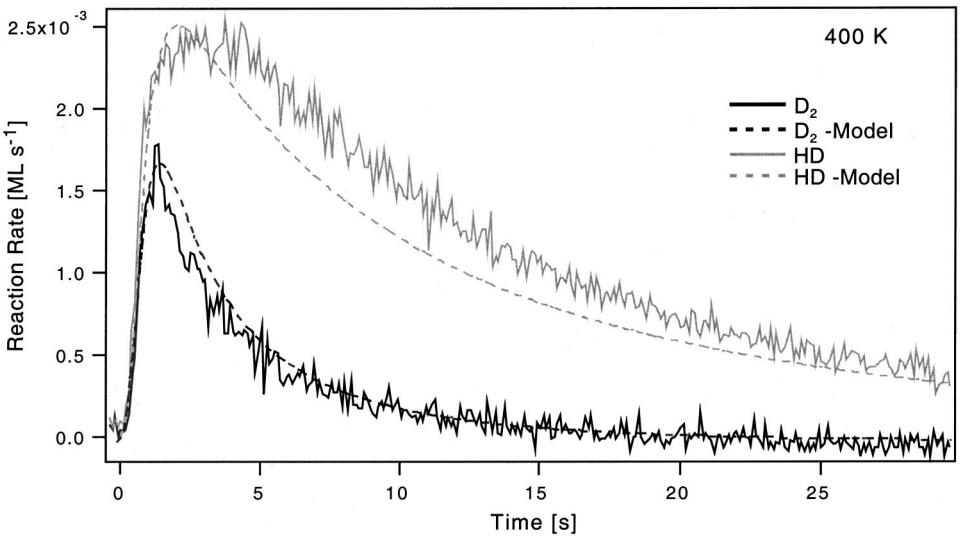

FIG. 15. Experimental (solid lines) and modeled (dashed lines) profiles of the D_2 and HD produced during the $CD_a + H_a$ reaction at a surface temperature of 400 K.

TABLE II. The frequencies for the normal modes of vibration for CH_a/CD_a on different transition metal surfaces determined using HREELS.

Crystal	ν_1:C-H(C-D)	ν_2:M-CH(M-CD)	$\nu_{3,4}$:C-H(C-D)
Ni{111} (Ref. 31)	2970(2220)	650(630)	1275(930)
Pd{100} (Ref. 34)	2940(2250)		925(715)
Rh{111} (Ref. 35)	2930(2220)		930
Pt{111} (Ref. 6)	2955		770
Pt{111} (Ref. 27)	2960(2220)		795(590)

Arrhenius analysis to determine the activation energy and pre-exponential factor for exchange. The best fit was obtained with $k_1/k_{-1}=3.0$. We obtain an estimate for the activation energies in each direction by *assuming* the same pre-exponential factor for H_2 and D_2 and for the forward and reverse surface reactions. This yields the activation energies for the CH_a+D_a reaction of 70 kJ mol^{-1} and for the CD_a+H_a reaction of 73.2 kJ mol^{-1}. These values compare favorably to the DFT slab calculations values derived by Michaelides and Hu on Pt{111}[11] and by Nørskov and co-workers on Ni{111}[12] of 94 kJ mol^{-1} and 70 kJ mol^{-1}, respectively. A higher pre-exponential factor would give an activation energy closer to that calculated by Michaelides and Hu.

B. Theoretical estimation of the kinetic isotope effect

We have shown that the exchange process is described by the following equilibrium:

$$CH_a+D_a \underset{k_{-1}}{\overset{k_1}{\rightleftharpoons}} CD_a+H_a. \tag{13}$$

We will assume that exchange occurs in both directions via a CHD_a transition state. We can therefore use transition state theory to determine the rate constant, in either direction, from the properties of the reactants and the transition state.[28–30] The KIE which is the ratio of the rate constants is given by the following expression:

$$\frac{k_1}{k_{-1}}=\frac{Q_{CD}Q_H}{Q_{CH}Q_D}e^{\Delta E/k_BT}, \tag{14}$$

where

$$\Delta E=+\sum_i \frac{1}{2}\frac{h\nu_{i(CH)}}{k_BT}+\sum_i \frac{1}{2}\frac{h\nu_{i(D)}}{k_BT}-\sum_i \frac{1}{2}\frac{h\nu_{i(CD)}}{k_BT} -\sum_i \frac{1}{2}\frac{h\nu_{i(H)}}{k_BT} \tag{15}$$

is the difference in zero point energy between the reactants and the products, summing over all the vibrational modes, and Q_X is the total partition function of species X.

In our present analysis a rigid solid surface is assumed: the surface partition functions are unity. We also assume that the reactants and transition states are localized on the surface. The total partition function is equated to the total vibrational partition function, Q_{vib}. To evaluate Q_{vib} it was assumed that both the frustrated rotational and vibrational bending modes are doubly degenerate and have the same frequency as on the {111} surface, as shown in Table II. A value for the metal–carbon stretch was taken from Ni{111} data;[31] HREELS studies on other isotopically substituted hydrocarbon fragments show that the metal–carbon stretching frequency is not changed significantly by isotopic substitution of H in CH_{xa}, where $x=0-3$. A reduction in frequency of about 20 cm^{-1} when H is replaced by D is typical. Frequencies for the frustrated translations ν_5 and ν_6 have not been experimentally determined for CH_a. A frequency of 200 cm^{-1} was chosen for the two frustrated translation modes ν_5 and ν_6. Since the change in frequency which occurs after isotopic substitution is the frequency ratio[32]

$$\frac{\nu_{5,6(CH)}}{\nu_{5,6(CD)}}=\left(\frac{M_{(CD)}}{M_{(CH)}}\right)^{1/2}, \tag{16}$$

where $M_{(CH)}$ and $M_{(CD)}$ are the masses of CH and CD, respectively, the contribution to the calculated KIE is insensitive to the absolute choice of frequency.

TABLE III. Partition functions for the individual vibrational modes, total partition functions, and total zero point energies for the exchange reaction at a surface temperature of 400 K.

Species	q_1	q_2	q_3	q_4	$q_{5,6}$	Q_X	$\sum_i \frac{1}{2}\frac{h\nu_i}{k_BT}$
CH_a	1	1.106	1.061	1.061	1.947	4.72	10.089
CD_a	1	1.115	1.135	1.135	1.995	5.72	7.956
H_a	1.013	1.198	1.198			1.45	3.964
D_a	1.041	1.310	1.310			1.79	3.062

Since Pt–H stretching frequencies for adsorbed H_a on Pt{110} are not available, frequencies were obtained from data for the Pt{111} surface: Bruchmann and co-workers[33] found ν_1(Pt–H) and (Pt–D) to be at 1200 and 900 cm^{-1}, respectively, and the $\nu_{2,3}$ and (Pt–H) and (Pt–D) to be 500 and 400 cm^{-1}, respectively. These frequencies were used to calculate the total partition functions, shown in Table III. The total zero point energy for each species is also included.

We estimate the kinetic isotope effect using Eq. (14) to be 3.36, which agrees very well with the value of 3.0 obtained by fitting the model to the experimental data. Therefore we conclude that QM tunneling is not significant for the exchange reaction at 400 K.

V. SUMMARY AND CONCLUSION

The D_2 exchange of H in CH_a was found to be extremely facile at a surface temperature of 350 K. The exchange occurs via a Langmuir–Hinshelwood reaction between a D_a atom and a CH_a fragment, to produce HD and H_2. The reaction rate is quite insensitive to the reaction temperature over the surface temperature range studied (370–420 K), which suggests a low activation energy.

Surface CH_a is completely deuterated to CHD_3 and CD_4 at a high D_2 flux of 1.2 ML s^{-1}, and the process can be ascribed to a stepwise deuteration mechanism.

The reverse exchange reaction, CD_a+H_a, was found to occur at about half the rate. The exchange process is successfully modeled using a system of four coupled differential equations, which describe the rate of change of the adsorbate coverages. Finally, the difference in rate between the forward

and reverse reactions is readily attributed to zero point energy differences; quantum mechanical tunneling of H/D need not be invoked.

ACKNOWLEDGMENTS

The authors acknowledge an equipment grant from the UK EPSRC, a TMR Studentship from the European Community (D.T.P.W.) and EPSRC postdoctoral support (Q.G.).

[1] F. Fischer and H. Tropsch, Brennst. Chem. **7**, 97 (1926).
[2] F. Fischer and H. Tropsch, Chem. Ber. **59**, 830 (1926).
[3] F. Zaera, Surf. Sci. **262**, 335 (1992).
[4] F. Zaera, Langmuir **7**, 1998 (1991).
[5] F. Zaera and H. Hoffmann, J. Phys. Chem. **95**, 6297 (1991).
[6] M. A. Henderson, G. E. Mitchell, and J. M. White, Surf. Sci. **184**, L325 (1987).
[7] Z. M. Liu, S. Akhter, B. Roop, and J. M. White, J. Am. Chem. Soc. **110**, 8708 (1988).
[8] D. H. Fairbrother, X. D. Peng, M. Trenary, and P. C. Stair, J. Chem. Soc., Faraday Trans. **91**, 3619 (1995).
[9] D. H. Fairbrother, X. D. Peng, R. Viswanathan, P. C. Stair, M. Trenary, and J. Fan, Surf. Sci. Lett. **285**, L455 (1993).
[10] D. T. P. Watson, S. Titmuss, and D. A. King, Surf. Sci. (in press).
[11] A. Michaelides and P. Hu (unpublished).
[12] R. M. Watwe, H. S. Bengaard, J. R. RostrupNielsen, J. A. Dumesic, and J. K. Nørskov, J. Catal. **189**, 16 (2000).
[13] C. T. Rettner, H. E. Pfnür, and D. A. Auerbach, Phys. Rev. Lett. **54**, 2716 (1985).
[14] M. M. McMaster and R. J. Madix, Surf. Sci. **275**, 265 (1992).
[15] J. Harris and A. C. Luntz, Surf. Sci. **287/288**, 56 (1993).
[16] M. Yata and R. J. Madix, Surf. Sci. **328**, 171 (1995).
[17] D. T. P. Watson, J. J. W. Harris, and D. A. King, Surf. Sci. (in press).
[18] V. A. Ukraintsev and I. Harrison, Surf. Sci. Lett. **286**, L571 (1993).
[19] A. Hopkinson, X.-C. Guo, J. M. Bradley, and D. A. King, J. Chem. Phys. **99**, 1 (1993).
[20] D. A. King and M. G. Wells, Surf. Sci. **29**, 454 (1972).
[21] A. V. Walker, B. Klotzer, and D. A. King, J. Chem. Phys. **109**, 6879 (1998).
[22] A. V. Walker and D. A. King, J. Chem. Phys. **112**, 4739 (2000).
[23] T. E. Jackman, J. A. Davies, D. P. Jackson, W. N. Unertl, and P. R. Norton, Surf. Sci. **120**, 389 (1982).
[24] J. R. Engstrom, W. Tsai, and W. H. Weinberg, J. Chem. Phys. **87**, 3104 (1987).
[25] Unpublished work performed in one of the author's (D.A.K.) laboratory at Cambridge.
[26] X. C. Guo and D. A. King, Surf. Sci. Lett. **302**, L251 (1994).
[27] M. Y. Smirnov, V. V. Gorodetskii, A. R. Cholach, and D. Y. Zemlyanov, Surf. Sci. **311**, 308 (1994).
[28] K. J. Laidler, *Chemical Kinetics*, 3rd ed. (Harper and Row, New York, 1987).
[29] S. Glasstone and E. H. Laidler, *The Theory of Rate Processes* (McGraw-Hill, New York, 1941).
[30] M. A. van Daelen, Y. S. Li, J. M. Newsam, and R. A. van Santen, J. Phys. Chem. **100**, 2279 (1996).
[31] M. B. Lee, Q. Y. Yang, and S. T. Ceyer, J. Chem. Phys. **87**, 2724 (1987).
[32] H. Ibach and D. L. Mills, *Electron Energy Loss Spectroscopy and Surface Vibration*, (Academic, New York, 1982).
[33] A. M. Baro, H. Ibach, and H. D. Bruchmann, Surf. Sci. **88**, 384 (1979).
[34] E. M. Stuve and R. J. Madix, J. Phys. Chem. **89**, 105 (1985).
[35] B. E. Koel, J. E. Crowell, B. E. Bent, C. M. Mate, and G. A. Somorjai, J. Phys. Chem. **90**, 2949 (1986).